Modulation of PDO on the predictability of the interannual variability of early summer rainfall over south China

Wansuo Duan,[1] Linye Song,[1,2] Yun Li,[3] and Jiangyu Mao [1]

Received 18 March 2013; revised 3 October 2013; accepted 18 October 2013.

[1] This study investigates the modulation of the Pacific Decadal Oscillation (PDO) on the predictability of interannual early summer south China rainfall (SCR) using high-quality station rainfall data. Of particular interest is the difference in impact between negative and positive phases of the PDO on the predictability of interannual early summer SCR. A clear difference in the correlation between the interannual early summer SCR and the preceding sea surface temperature (SST) over the Pacific Ocean appears in negative and positive phases of the PDO. In the negative PDO phase, the correlation between interannual early summer SCR and SST is dominated by a pattern with significant negative correlations in the subtropical western North Pacific and southeast Pacific and significant positive correlations in the tropical central Pacific. However, in the positive PDO phase, significant positive correlations are observed in the tropical eastern Pacific. It is found that, for each PDO phase, the preceding SST anomalies in some regions in the Pacific may act as predictors of the interannual early summer SCR. As such, a two-regime regression model for the relationship between interannual early summer SCR and preceding SST anomalies is established based on the negative and positive PDO phases using respective multiple linear regression models. Results suggest that the interannual early SCR is more predictable in PDO positive phase than in negative phase. It offers a support for the argument that a segmented statistical forecasting approach associated with the decadal modulation effect of the coupled ocean atmospheric mode should be adopted to forecast the early summer SCR.

Citation: Duan, W., L. Song, Y. Li, and J. Mao (2013), Modulation of PDO on the predictability of the interannual variability of early summer rainfall over south China, *J. Geophys. Res. Atmos.*, *118*, doi:10.1002/2013JD019862.

1. Introduction

[2] Studies showed that the East Asian summer climate experienced significant interdecadal changes. Specifically, in the Yangtze River region, a major abrupt change of increased summer rainfall was observed in the late 1970s [*Yatagai and Yasunari*, 1994; *Wu and Chen*, 1998; *Gong and Ho*, 2002; *Qian and Qin*, 2008]; and in the Yellow River region, the increased July rainfall was also observed during the middle and by the end of the 1970s and occurred a significant interdecadal change [*Hu et al*., 1993]. However, in south China (SC), which is located at the southern margin of East China and receives the bulk of its annual rainfall during flooding season in summer [*Wu et al*., 2012], the summer rainfall was characterized by a pronounced interdecadal change with rainfall anomalies changed from above normal to below normal in the late 1970s [*Nitta and Hu*, 1996; *Hu*, 1997]. Furthermore, another decadal change of increased summer rainfall over SC can also be observed around 1992/1993, but with increased rainfall [*Ding et al*., 2008; *Wu et al*., 2010].

[3] The reasons for interdecadal changes of the East Asian summer climate are complex. The abrupt change in the late 1970s concurred with the well-known climate shift, with large-scale interdecadal variations in sea surface temperature (SST) and atmospheric circulation over the tropical and extratropical Pacific [*Miller et al*., 1994; *Zhang et al*., 1997]. This change was directly characterized with the intensification and westward and southward extension of the western Pacific subtropical high (WPSH) and also largely influenced by the change of SST anomalies and convection activity in the tropical Indian Ocean and western Pacific Ocean [*Hu*, 1997; *Zhou et al*., 2009]. Other contributions such as the Tibetan Plateau snow were also suggested [*Chen and Wu*, 2000; *Zhang et al*., 2004]. In addition, the rainfall significantly increase around 1992/1993 was linked to an increase in lower-level convergence, midtropospheric ascent, and upper level divergence over SC [*Wu et al*., 2010].

[4] The Pacific Decadal Oscillation (PDO) is the strongest decadal oscillatory signal in the Pacific [*Mantua et al*., 1997; *Mantua*, 2002]. Previous studies suggested that the PDO has an interdecadal modulation effect on the global climate

[1]State Key Laboratory of Numerical Modeling for Atmospheric Sciences and Geophysical Fluid Dynamics, Institute of Atmospheric Physics, Chinese Academy of Sciences, Beijing, China.
[2]University of Chinese Academy of Science, Beijing, China.
[3]CSIRO Computational Informatics, CSIRO Climate Adaptation Flagship, Wembley, Western Australia, Australia.

Corresponding author: W. Duan, State Key Laboratory of Numerical Modeling for Atmospheric Sciences and Geophysical Fluid Dynamics, Institute of Atmospheric Physics, Chinese Academy of Sciences, Beijing 100029, China. (duanws@lasg.iap.ac.cn)

2169-897X/13/10.1002/2013JD019862

[*Gershunov and Barnett*, 1998; *Power et al*., 1999; *Hu and Huang*, 2009; *Silva et al*., 2011; *Kim et al*., 2013] through modulating the El Niño–Southern Oscillation (ENSO)-related teleconnections. For the local region of SC, *Chan and Zhou* [2005] investigated the modulation of PDO on the SC rainfall. They demonstrated that the early summer monsoon rainfall over SC tends to be below or above normal more often when the ENSO and PDO are in phase, while the rainfall has no wet or dry preference when the ENSO and PDO are out of phase. *Mao et al*. [2011] further suggested that interannual variations of the early summer monsoon rainfall over SC are significantly modulated by the interdecadal fluctuations of PDO. Their results suggest that the dominant atmospheric teleconnection patterns associated with extremely wet and dry rainfall conditions are remarkably different during the periods 1958–1976 and 1980–1998. It is hypothesized that different "background" PDO conditions (i.e., PDO positive and negative phases) may first affect the ENSO-related SST anomalies, especially the SST anomalies over the western North Pacific and the Philippine Sea, and then affect the early summer monsoon rainfall over SC through modifying the intensity of the subtropical high [*Chan and Zhou*, 2005].

[5] Since the PDO influences the ENSO-related SST anomalies and the changing of ENSO-related SST anomalies may largely contribute to the interannual variation of early summer south China rainfall (SCR), we speculate that the PDO may modulate the predictability of the interannual variation of the early summer SCR by influencing the ENSO-related SST anomalies. If so, corresponding statistical forecast models of the interannual early summer SCR should be respectively established under different "background" PDO conditions (i.e., the PDO positive and negative phases), according to the respective relationship between the interannual early summer SCR and the preceding SST anomalies. The so-called predictability here is referred to the prediction skill of the interannual early summer SCR estimated by the statistical models.

[6] There are some efforts made to forecast the rainfall in China by using statistical models. For example, *Zhang et al*. [2011] developed a statistical forecasting model based on partial least squares (PLS) regression by using SST anomalies in the preceding October to predict the occurrence of an anomalous wet and cold January in SC. They succeeded in hindcasting the January 2008 severe freezing precipitation event; furthermore, they revealed a significant shift of the dominant SST patterns responsible for the climatic anomalies in the periods of 1949–1978 and 1978–2007. *Guo et al*. [2012] built a time scale decomposition (TSD) approach to statistically downscale the summer rainfall in north China by identifying influencing factors linked to the interdecadal and interannual variabilities, respectively. Their results showed that the TSD approach was acceptable to predict the observed rainfall. Nevertheless, the TSD approach is based on an assumption that the interannual variation of rainfall in China is not modulated by an interdecadal climate background. As mentioned above, the coupled ocean atmosphere mode on interdecadal time scale may exert a modulation on the interannual rainfall in China [*Chan and Zhou*, 2005; *Zhou and Chan*, 2007; *Zhou et al*., 2007; *Lin et al*., 2010; *Mao et al*., 2011; *Zhu et al*., 2011]. The relationship between the preceding SST and interannual early summer SCR may be different in positive and negative phases of the PDO, and hence, the corresponding statistical models of the interannual early summer SCR should not be same. These speculations motivate us to explore whether or not the PDO modulates the predictability of the interannual variability of the early summer SCR with an aim to answer the following questions:

[7] 1. Can the preceding SST anomalies act as a predictor of the interannual variability of early summer SCR?

[8] 2. Are the SST-related predictors the same in positive and negative phases of the PDO? If not, what are the differences?

[9] 3. Under which phase of PDO is the predictability of the interannual variability of the early summer SCR higher?

[10] The paper is organized as follows. In section 2, we introduce the data sets used in this study. Section 3 displays the variations of early summer SCR and investigates the associated atmospheric circulation anomalies in different PDO phases. In section 4, we explore the SST-related predictors in the training period that can be potentially used to predict the interannual early summer SCR for negative and positive phases of the PDO, respectively. In section 5, we use the predetermined SST-related predictors to build statistical forecasting models of the interannual early summer SCR using the multiple linear regression (MLR) approach and examine the predictabilities of the interannual early summer SCR in the two phases of the PDO. Finally, discussion and summary are presented in sections 6 and 7, respectively.

2. Data

[11] Winds and vertical velocity were extracted from the National Centers for Environmental Prediction-National Center for Atmospheric Research (NCEP-NCAR) reanalysis data set. This data set has a horizontal resolution of 2.5° × 2.5° and is available from 1948 to the present [*Kalnay et al*., 1996]. The SST data used in this study are taken from the National Oceanic and Atmospheric Administration (NOAA) Extended Reconstruction SST, version 3 [*Smith et al*., 2008], on a 2.0° × 2.0° grid from 1854 to the present, which can be downloaded from the NOAA web site (http://www.esrl.noaa.gov/psd/data/gridded/).

[12] The PDO index is defined as the leading principle component (PC) from an unrotated empirical orthogonal function analysis of monthly "residual" SST anomalies in the North Pacific Ocean, poleward of 20°N [*Mantua et al*., 1997], and "residual" here means removing the monthly mean global average SST anomalies to separate the PDO pattern of variability from any "global warming" signal [*Zhang et al*., 1997]. The values for the PDO index used here are taken from the Joint Institute for the Study of the Atmosphere and Ocean at their website http://jisao.washington.edu/pdo/PDO.latest, which contains data from 1900 to the present. The Niño 3.4 index was downloaded from the NOAA web site (http://www.cgd.ucar.edu/cas/catalog/climind/TNI_N34/index.html#Sec5).

[13] The rainfall data analyzed here were used by *Mao et al*. [2011] and *Chan and Zhou* [2005], including monthly rain gauge observations at Guangzhou (23.08°N, 113.16°E), Hong Kong (22.11°N, 114.14°E), and Macao (22.16°N, 113.35°E) for the period 1910–2011, provided by the respective weather bureaus. In addition, monthly mean precipitation at 160 Chinese stations since 1951 provided by the China Meteorological Administration (CMA) was also employed in this study. These station observations are operated by the

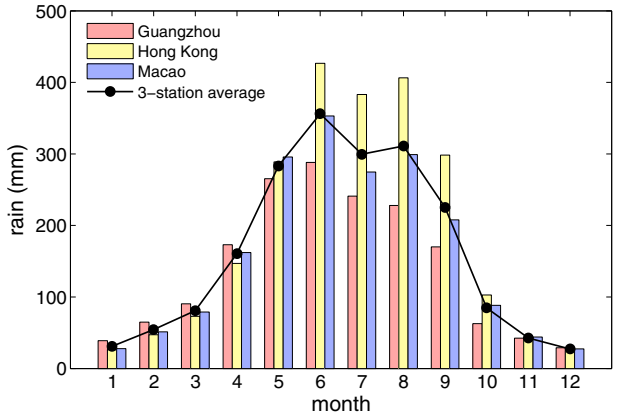

Figure 1. The annual climatological cycle of the rainfall at the stations of Guangzhou, Hong Kong, and Macao and the three-station average, which is estimated using the rainfall data during 1910–2011.

CMA consistently through the observation period, meeting the standards of the World Meteorological Organization.

3. Early Summer SCR and Related Atmospheric Circulation Anomalies in Different PDO Phases

[14] Figure 1 shows the climatological annual cycles of the rainfall at the stations of Guangzhou, Hong Kong, and Macao averaged over the 1910–2011 period. The patterns at each of the stations all display a bimodal distribution, with the maximum rainfall in June and a second maximum in August. The rainfall increases slowly before April but increases rapidly starting in May, coinciding with the onset of the South China Sea summer monsoon (SCSSM), which generally occurs in mid-May [*Zhou and Chan*, 2007]. After September, the rainfall decreases rapidly, and there is much less precipitation in winter.

[15] During the summer rainy season (June to August), rainfall anomalies can be caused by various factors, such as the summer monsoon, tropical cyclones (TCs), rainstorms, local topography and other rainfall events that are not associated with distinct weather systems [*Wu et al*., 2012]. As indicated by *Zhou et al*. [2006], the SCR increasing again in August (Figure 1) is attributed to the activity of TCs, which could bring a large amount of rainfall. *Wu et al*. [2012] also identified two typical rainy seasons over SC: one occurs in early summer, and the other occurs in late summer. The rainfall in early summer is mainly related to summer monsoon activity, while the rainfall in late summer is partly due to TCs. Because of the "hybrid" nature of the rain-bearing system in the late summer over SC and the peak rainfall that happens in June, we focus on June rainfall (i.e., early summer SCR) in this study. In other words, in the present study we are mainly concerned with pure summer monsoon rainfall over SC.

[16] Figure 2 displays the simultaneous detrended correlation pattern between time series of the three-station (Guangzhou, Hong Kong, and Macao) averaged rainfall in June and those June rainfall gauged at 160 stations over the period 1951–2011. It is evident that a significant positive correlation pattern at the 99% confidence level appears over SC (specifically, the region east of 105°E and south of 25°N). As a result, June rainfall averaged over these three stations can act as a representative of the early summer rainfall over SC region, called the early summer SCR. The time series of June rainfall averaged over these three stations in the period 1910–2011 is further used as the long term early summer SCR.

[17] Figure 3 shows the time series of the standardized early summer SCR and its interdecadal variations represented by 11-year running mean. The interdecadal variability of the early summer SCR agrees well with that of the PDO index, which is estimated by taking the average of the PDO index from March to June (MAMJ) and its interdecadal variability is also filtered using an 11-year running mean. The MAMJ PDO index is preferred because we analyze the relationship between preceding monthly SST from March to May and the early summer June rainfall in this study. As shown in Figure 3, the interdecadal variations of early summer SCR tends to have negative (positive) anomalies during the period of positive (negative) PDO phase. The correlation coefficient between the interdecadal SCR and the PDO reaches −0.63, which is statistically significant at the 95% confidence level after reducing the degrees of freedom caused by the running mean. Indeed, the effective degrees of freedom $N^{\text{eff}} = 9$ and the critical correlation value $R_{0.05} = 0.60$ [*Davis*, 1976; *Chen and Chen*, 2011]. Therefore, the negative phase of PDO is inclined to coincide with abundant summer rainfall over SC, while the positive phase of PDO tends to be associated with the reduction of rainfall. This result is consistent with the findings of previous studies [*Chan and Zhou*, 2005; *Zhou et al*., 2006] that the interdecadal variability of the early summer SCR is closely related to the PDO phases, with above-normal (below-normal) rainfall anomalies in the negative (positive) phase of PDO. An intuitive question is whether the interannual variability component of the early summer SCR is related to the negative and positive phases of PDO. Especially, is the predictability of the interannual variation of early summer SCR modulated by the PDO? This is important for exploring the predictability of the early summer SCR, which is a central issue of the present study.

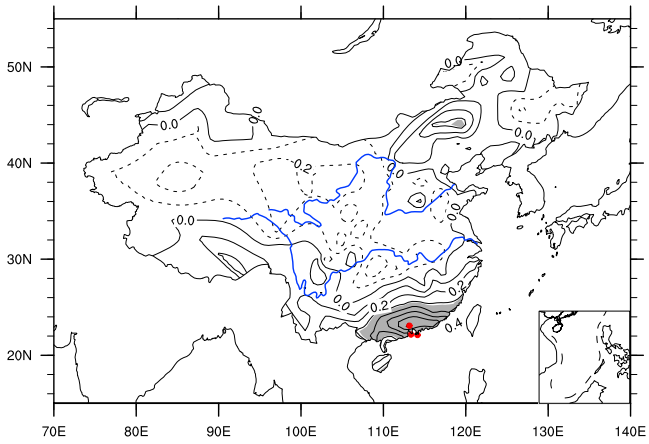

Figure 2. Correlation of the detrended three-station averaged June rainfall with the China 160-station June rainfall during the period 1951–2011. Grey shading indicates correlation coefficient significant at the 99% confidence level based on a *t* test. The stations at Guangzhou, Hong Kong, and Macao are indicated by three red dots.

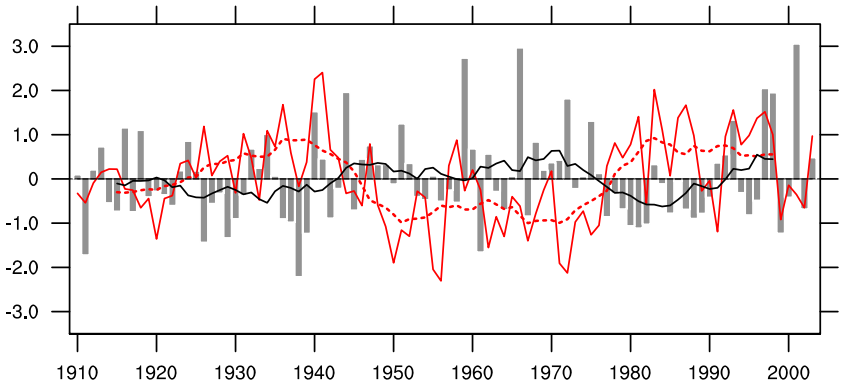

Figure 3. Standardized time series of the early summer SCR (bar) and its 11-year running mean (solid black curve) as well as a standardized time series of March to June averaged PDO index (solid red line) and its 11 year running mean (dashed red line).

[18] The PDO shows three transition years between negative and positive phases approximately around 1924/1925, 1946/1947, and 1976/1977 (Figure 3), which are consistent with those identified by *Mantua et al*. [1997], especially with the well-known climate shift that happened in the late 1970s from a negative to positive PDO phase. To explore the modulation of PDO on the predictability of the interannual early summer SCR, the periods of positive and negative phases of the PDO are selected. Considering the accuracy of data and the length of the NCEP-NCAR reanalysis data, we choose the recent two periods of 1948–1976 and 1977–1998 to compare the predictabilities throughout this study. These two periods correspond to a negative and a positive PDO phase and present a significant PDO signal in recent past decades, which is favorable for identifying the differences between the predictabilities of the interannual early summer SCR in the positive phase of PDO and those in the negative phase.

[19] To explore the modulation of PDO on the interannual variation of early summer SCR, the atmospheric circulation anomalies associated with the interannual early summer SCR in negative (1948–1976) and positive (1977–1998) PDO phases are first examined. The interannual variation of early summer SCR was extracted by using 11-year high pass filters [*Zhang et al*., 1997; *Garreaud and Battisti*, 1999]. Figure 4 shows the anomalies of winds and vertical p velocity regressed onto the interannual early summer SCR. In the negative PDO phase, low-level winds at 850 hPa display an anomalous anticyclone over the Philippine Sea and South China Sea (SCS) and an anomalous cyclone over SC, leading to convergence along the southeastern coast of China. Thus, moisture from the SCS can be transported to the SC region by the southwesterlies and so favors increasing rainfall in SC (Figure 4a). Meanwhile, another anomalous anticyclone is also observed over Northeast China and Japan, extending to 60°N. Thus, during the negative PDO phase, the wind anomalies feature a meridional wave train from the SCS and Philippine Sea to the Sea of Okhotsk (Figure 4a). Such a meridional juxtaposition of anomalous circulations is advantageous to increasing the early summer SCR [*Mao et al*., 2011]. Additionally, significant southwesterlies appear over northeast Australia, which may indicate strong interaction between the Northern and Southern Hemisphere through the cross-equatorial flows [*Xue et al*., 2003a; *Xue and He*, 2005]. In this case, the influence of anomalous circulation in the Southern Hemisphere on the Asian summer monsoon is mainly through the cross-equatorial flow, and strong cross-equatorial flow increases the activity of the summer monsoon in Northern Hemisphere, finally favoring summer rainfall in China, especially in SC [*Xue et al*., 2003b]. The vertical motion at 500 hPa displays anomalous ascent over SC but anomalous descent over northern Philippines (Figure 4b). That is, the vertical motion acts on the southwesterly transported moisture and drives the moisture upward, encouraging the formation of rainfall. *Wu et al*. [2012] suggested that the meridional wave train pattern from the SCS and Philippine Sea to the Sea of Okhotsk may significantly influence summer SCR. It is demonstrated that the distinct wave train emanates from the tropical western Pacific by the Pacific-Japan pattern [*Nitta*, 1987, 1989], which is also named as the East Asian-Pacific teleconnection [*Huang and Li*, 1987].

[20] In the positive PDO phase, the anomalous atmospheric circulation associated with the interannual SCR is different from that in the negative PDO phase. Specifically, the meridional wave train from the SCS and Philippine Sea to the Sea of Okhotsk related to the negative PDO phase disappears in the positive phase (Figure 4c). The lack of meridional wave train may lead to the weakening of the vertical easterly shear over the tropical western North Pacific in June, which is unfavorable for coupling and thus weakens the meridional teleconnection [*Lin et al*., 2010]. As shown in Figure 4c, remarkable westerly anomalies dominate the central and eastern tropical Pacific, which are hardly observed in the negative PDO phase. Although the low-level winds at 850 hPa also show an anomalous anticyclone over the SCS, it is located more westward and southward than that in the negative PDO phase. The vertical motion anomalies at 500 hPa show ascent over SC and descent over the Maritime Continent. Furthermore, there is a robust ascent over the tropical eastern Pacific (Figure 4d), which is not observed in the negative PDO phase. Under such circumstances, the Walker circulation is weakened and an anomalous anticyclone in the SCS could be induced through the Pacific-East Asian teleconnection [*Wang et al*., 2000]. This anticyclonic anomaly guides southwesterly flows in its northwestern edge to transport moisture from the SCS to the SC region and then acts on the ascent motion, finally increasing early summer rainfall over SC.

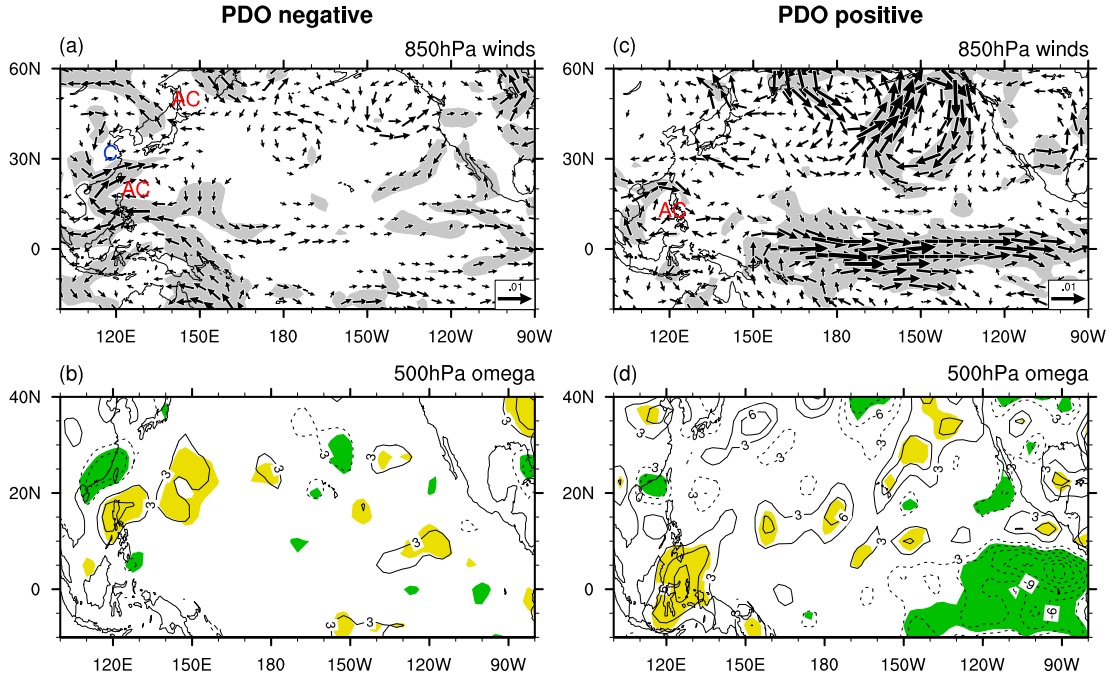

Figure 4. Anomalies of (a, c) horizontal winds at 850 hPa and (b, d) p vertical velocity at 500 hPa regressed upon the interannual early summer SCR in negative (1948–1976, left) and positive (1948–1976, right) phases of the PDO. The regression is calculated only using the interannual component with an 11-year high pass filter. The shadings in Figures 4a–4d indicate significance at the 90% confidence level. The wind scale in Figures 4a and 4c is shown at the bottom right of the respective panels with units of 10^{-2} m s^{-1} mm^{-1}. The contour interval for the 500 hPa p vertical velocity is 3×10^{-5} Pa s^{-1} mm^{-1} in Figures 4b and 4d, and the zero contour is suppressed in Figures 4b and 4d. Anomalous anticyclones and cyclones are marked by "AC" and "A," respectively.

[21] The above analysis shows that the anomalous atmospheric circulation patterns associated with the interannual early summer SCR are remarkably different under negative and positive phases of the PDO. These anomalous atmospheric circulation conditions are linked to Pacific SST anomalies. As such, the relationship between the interannual early summer SCR and Pacific SST anomalies can be influenced by PDO phases. Born in mind of the persistence of SST, it motivated us to search the potential preceding SST predictors for the interannual early summer SCR separately in the negative and positive PDO phases, and then investigate the predictability of the interannual early summer SCR based on the selected SST predictors using statistical models.

4. The SST-Related Predictors of the Interannual Variability of Early Summer SCR

[22] In order to determine the potential SST predictors for developing statistical models for forecasting the interannual early summer SCR, we have split negative (1948–1976) and positive (1977–1998) phases into training and testing periods: 1948–1968 (1977–1992) for the training period of the negative (positive) PDO phase, while the 1969–1972 (1993–1998) for the testing period of the negative (positive) PDO phase. Only the respective training periods of 1948–1968 and 1977–1992 are used for identifying the potential SST predictors for PDO negative and positive phases, respectively.

[23] Figure 5 shows the correlation patterns of the interannual early summer SCR in the negative and positive PDO phases with the corresponding preceding SST by leading 1, 2, and 3 months in the respective training periods. It can be found that remarkable differences appear in the correlation patterns between positive and negative PDO phases, indicating that relations of interannual early summer SCR with preceding SST are significantly modulated by the PDO phases. In the negative PDO phase, negative correlations are observed in the subtropical western North Pacific and Southeast Pacific, and significant positive correlations are seen in the tropical central Pacific (Figures 5a–5c). However, in the positive PDO phase, although negative correlations can also be observed in the subtropical western North Pacific, the corresponding region is relatively much broad compared to that in the negative PDO phase except in April. Significant positive correlations are apparent in the equatorial eastern Pacific (Figures 5d–5f), basically covering the Niño 1+2 and Niño 3 regions, which cannot be found in the negative PDO phase. Therefore, the correlations between the interannual early summer SCR and the preceding Pacific SST are very different in the negative and positive PDO phases. Furthermore, several regions can be identified as having their SST significantly and consistently related to the early summer SCR in different month lags for the negative and positive PDO phases, respectively (Figure 5). This result indicates that the interannual variation of preceding SST anomalies in these key regions may explain the anomalous interannual early summer SCR to a larger extent than in other regions, i.e., the SST anomalies in these key regions could be regarded as potential predictors for the interannual variation of early summer SCR.

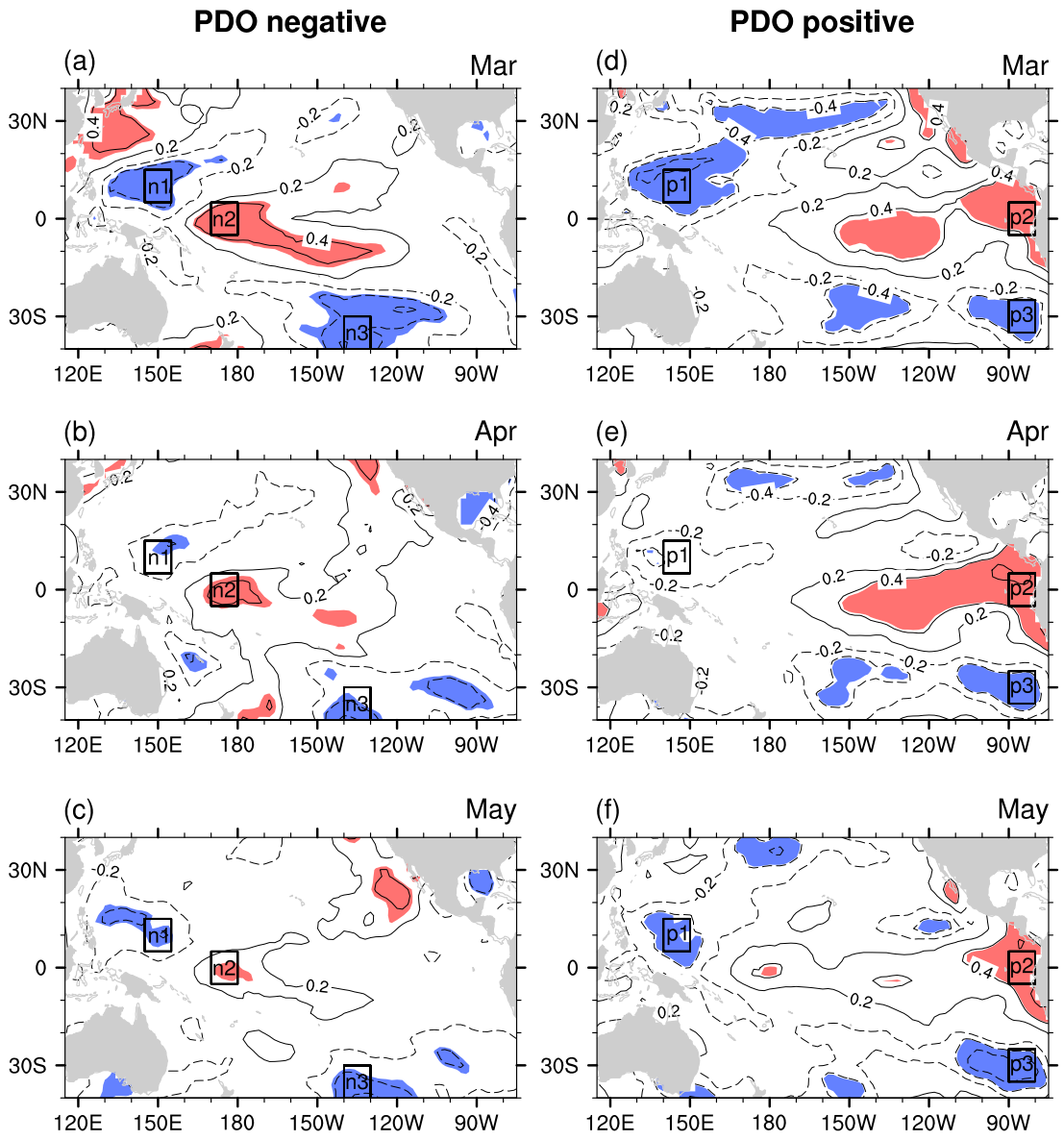

Figure 5. Correlation coefficients of the interannual early summer SCR with the Pacific SST in the preceding (a, d) March, (b, e) April, and (c, f) May, respectively, for (left) negative and (right) positive phases of the PDO in the training periods 1948–1968 and 1977–1992. Shadings in Figures 5a–5f indicate correlation coefficient significant at the 90% confidence level. The rectangles indicate the regions with high-correlation coefficients that are listed in Table 1. The linear trend and interdecadal variability are removed. The correlation is calculated only by using the interannual component with an 11-year high pass filter.

[24] To check the robust relationship between the SCR and SST, a filed significance test proposed by *Livezey and Chen* [1983] based on Monte Carlo simulations are employed to evaluate the field significance of correlation patterns in Figure 5. The rainfall time series was replaced with a random time series sampled from a Gaussian distribution N(0,1). Then, correlation between this random time series and the Pacific SST are obtained at every grid point and tested for significance. This experiment is completed a total of 1000 times with different random inputs and all results are presented in Figure 6. For the correlation pattern in March during the PDO negative (positive) phase, the shadings in Figure 5a (5d) represents 17.7% (20.4%) of the total area consisting of 3108 grid points. Because at least 10% of the trials have greater than 17.5% (17.9%) of their area statistically significant at the 90% confidence level, the hypothesis that the result shown in Figure 5a (5d) is a chance occurrence can be rejected at the 90% confidence level (Figures 6a and 6d). That is to say, they are significant fields at the 90% confidence level. Although the correlation patterns in April and May for both PDO negative and positive phases are not field significant at the 90% confidence level (Figures 6b, 6c, 6e, and 6f), these correlation patterns show a consistent temporal evolution with the changing of lag months in both PDO negative (Figures 5a–5c) and positive phase (Figures 5d–5f), implying that they may not be due to a random phenomenon.

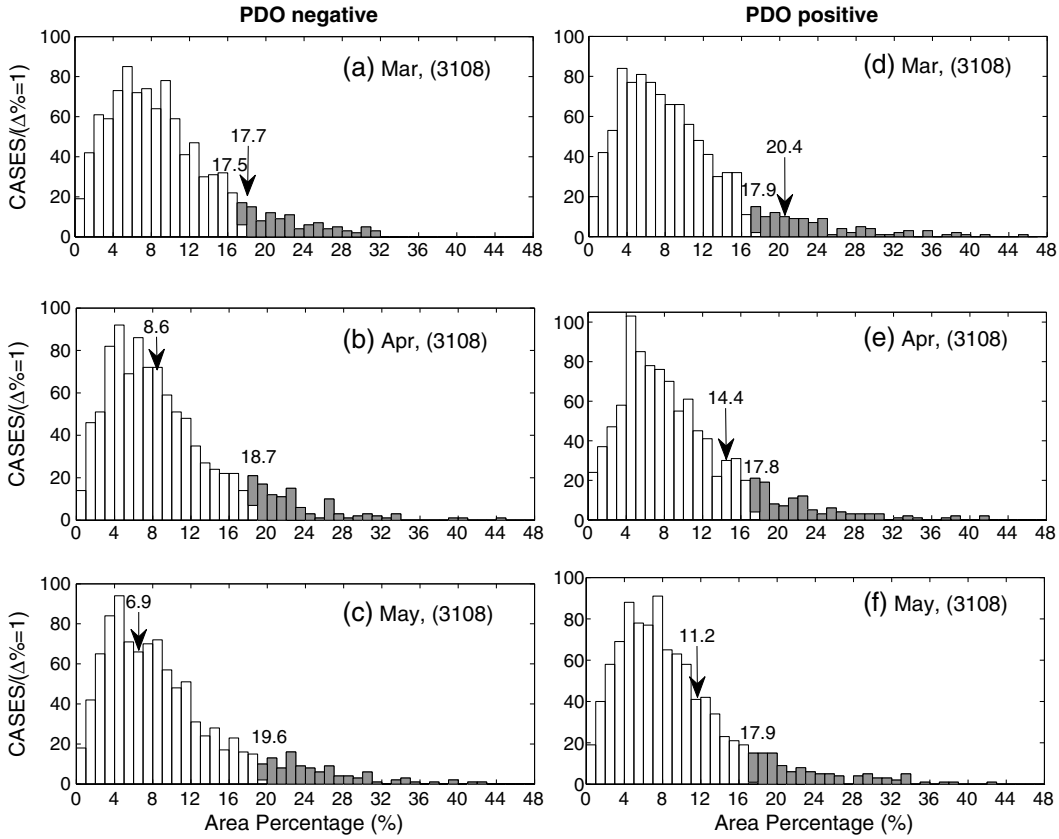

Figure 6. Histograms of percent of area with correlations of preceding Pacific SST and Gaussian noise statistically significant at the 90% confidence level in 1000 Monte Carlo trials. The abscissa is percent of area while the ordinate is number of cases for each 1% interval. The 10% tail is schematically shown by shading the 100 of 1000 largest percents. The results for correlations with early summer SCR in Figure 4 are shown by vertical arrows.

Hence, the SST patterns in April and May are also included as potential predictors for the interannual early summer SCR.

[25] The above results demonstrated that the interannual early summer SCR is much closely related to the SST anomalies in the selected box regions n_i and p_i (i = 1, 2, 3; Figure 5) than those in other regions. They may act as potential predictors of the interannual early summer SCR. These results stimulate the following questions: to what extent can the interannual early summer SCR be forecasted if we use the SST anomalies over the regions n_i and p_i in spring months (March, April, and May) to estimate the predictability of interannual early summer SCR? Are there any differences between the forecasting skill for interannual early summer SCR in the negative and positive PDO phases? Is it during the positive phase or negative PDO phase when the interannual early summer SCR has relatively stronger predictability? To address these questions, we use the preceding spring SST anomalies in the selected regions to build statistical models for the

Table 1. Correlation Coefficients Between the Interannual Early Summer SCR and SST Averaged Over Selected Regions of 10° Latitude and 10° Longitude in the Preceding Spring Months (March, April, and May) During the Training Period 1948–1968 for the Negative and 1977–1992 for the Positive PDO Phases, Respectively

PDO Negative Phase (Training Period)			PDO Positive Phase (Training Period)		
n_1 (5°N–15°N, 145°E–155°E)	$n_1\text{SST}_{\text{May}}$	−0.42[a]	p_1 (5°N–15°N, 140°E–150°E)	$p_1\text{SST}_{\text{May}}$	−0.45[a]
	$n_1\text{SST}_{\text{Apr}}$	−0.37[a]		$p_1\text{SST}_{\text{Apr}}$	−0.35
	$n_1\text{SST}_{\text{Mar}}$	−0.53[a]		$p_1\text{SST}_{\text{Mar}}$	−0.55[a]
n_2 (5°S–5°N, 170°E–180°E)	$n_2\text{SST}_{\text{May}}$	0.35	p_2 (5°S–5°N, 90°W–80°W)	$p_2\text{SST}_{\text{May}}$	0.55[a]
	$n_2\text{SST}_{\text{Apr}}$	0.41[a]		$p_2\text{SST}_{\text{Apr}}$	0.57[a]
	$n_2\text{SST}_{\text{Mar}}$	0.51[a]		$p_2\text{SST}_{\text{Mar}}$	0.50[a]
n_3 (30°S–40°S, 140°W–130°W)	$n_3\text{SST}_{\text{May}}$	−0.49[a]	p_3 (25°S–35°S, 90°W–80°W)	$p_3\text{SST}_{\text{May}}$	−0.67[a]
	$n_3\text{SST}_{\text{Apr}}$	−0.43[a]		$p_3\text{SST}_{\text{Apr}}$	−0.52[a]
	$n_3\text{SST}_{\text{Mar}}$	−0.51[a]		$p_3\text{SST}_{\text{Mar}}$	−0.52[a]

[a]Significant at the 90% confidence level.

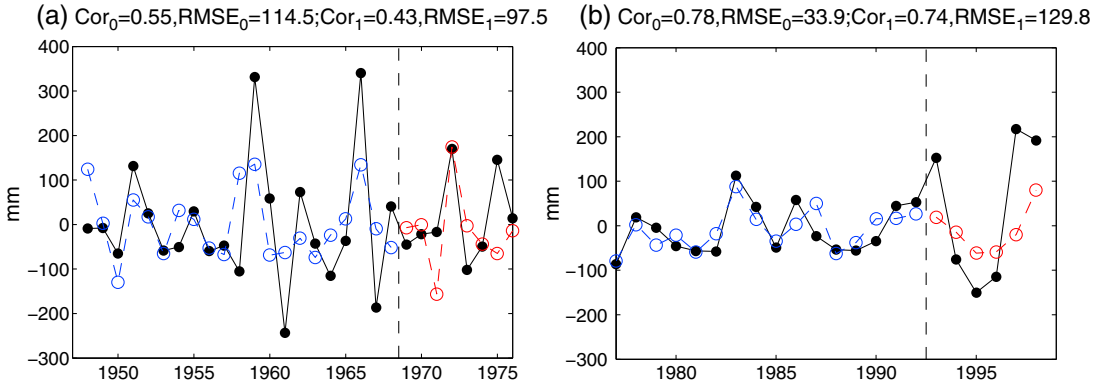

Figure 7. The results from the MLR model for interannual early summer SCR in (a) negative and (b) positive phases of the PDO, respectively. The solid line with filled circles is the observed interannual SCR time series; the dashed blue lines with unfilled circles are the reconstructed interannual rainfall time series; the dashed red lines with unfilled circles are the model forecasts of interannual rainfall. Cor_0 and $RMSE_0$ (Cor_1 and $RMSE_1$) in Figures 7a and 7b are the correlation and root-mean-square error (unit: mm) between the reconstructed (predicted) and observed interannual rainfall for the training (testing) period.

interannual early summer SCR based on the multiple linear regression (MLR) approach and then to estimate the interannual SCR predictability in the negative and positive PDO phases.

5. Statistical Models for the Relationship Between Interannual Early Summer SCR and the Preceding SST

[26] We have used the statistical correlation analysis to identify the key regions as having their SST significantly and consistently related to the early summer SCR in different month lags for the negative and positive PDO phases, respectively. To facilitate discussion, we denote these key regions of 10° latitude and 10° longitude as n_iSST for the negative PDO phase and p_iSST for the positive PDO phase (Figure 5). The preceding SST anomalies in March, April, and May averaged over the selected regions n_i are denoted as $n_i\mathrm{SST_{Mar}}$, $n_i\mathrm{SST_{Apr}}$, and $n_i\mathrm{SST_{May}}$ (i = 1, 2, 3) for the negative PDO phase. Similarly, $p_i\mathrm{SST_{Mar}}$, $p_i\mathrm{SST_{Apr}}$, and $p_i\mathrm{SST_{May}}$ (i = 1, 2, 3) are denoted as the SST anomalies averaged over the selected regions p_i in March, April, and May for the positive PDO phase. Table 1 lists the correlations between time series of interannual early summer SCR and preceding SST anomalies in March, April, and May during the training period.

[27] We use the region-averaged SST anomalies in preceding spring months (Table 1) to establish statistical models for interannual variations of early summer SCR using the Cross-Validation-Based Stepwise Regression Approach [*Guo et al.*, 2012]. For the negative PDO phase, a model for the relationship between the interannual early summer SCR and nine potential predictors ($n_i\mathrm{SST_{May}}$, $n_i\mathrm{SST_{Apr}}$, and $n_i\mathrm{SST_{May}}$, i = 1, 2, 3) was derived using the data over the training period from 1948 to 1968. The predicted values in the period 1969–1976 are chosen as the testing period to validate the forecasting skill of the model [*Li and Smith*, 2009]. For the positive PDO phase of 1977–1998, the training period is selected as 1977–1992, as in section 4, and the testing period is 1993–1998. This leads to two separated MLR models, which are respectively related to the interannual early summer SCR in negative and positive phases of the PDO:

$$\mathrm{SCR}_n = -321.4 \times n_1\mathrm{SST_{May}} + 121.7 \times n_2\mathrm{SST_{Apr}} - 4.7, \quad (1)$$

and

$$\mathrm{SCR}_p = -124.0 \times p_3\mathrm{SST_{May}} + 21.8 \times p_2\mathrm{SST_{Apr}} - 3.7, \quad (2)$$

where SCR_n and SCR_p represent the interannual SCR in negative and positive phases of the PDO, respectively. The MLR model of equation (1) is significant at the 95% confidence level (the F test value is 3.81 and exceeds the significant value of 3.52 at the 95% confidence level). While the MLR model of equation (2) is significant at the 99% confidence level (the F test value is 10.38 and exceeds the significant value of 6.51 at the 99% confidence level). In this situation, it is reasonable for us to adopt these two-regime models to conduct hindcast experiments for the interannual early summer SCR.

[28] Figures 7a and 7b compare the predicted and observed interannual early summer SCR by showing the associated correlation (Cor) and root-mean-square error (RMSE) in both PDO phases. In general, the performance of models in the training period is maintained in the testing period. It is shown that the two respective models show an acceptable forecast skill for the interannual early summer SCR, with the reconstructed correlation coefficient being 0.55 in the negative PDO phase and 0.78 in the positive PDO phase and the correlation coefficient between the observed and predicted rainfall reaching 0.43 in the negative PDO phase and 0.74 in the positive PDO phase in the testing period (Figures 7a and 7b). Also, it is obvious that the interannual early summer SCR in the positive PDO phase may have a relatively strong predictability compared to that in the negative PDO phase using the MLR approach based on the preceding SST predictors. This infers that the predictability of interannual early summer SCR is modulated by the PDO.

[29] We now give an interpretation of why the preferred predictors could be primarily responsible for the interannual early summer SCR variation. Figure 8 shows the regression map for low-level water vapor transport at 850 hPa and p

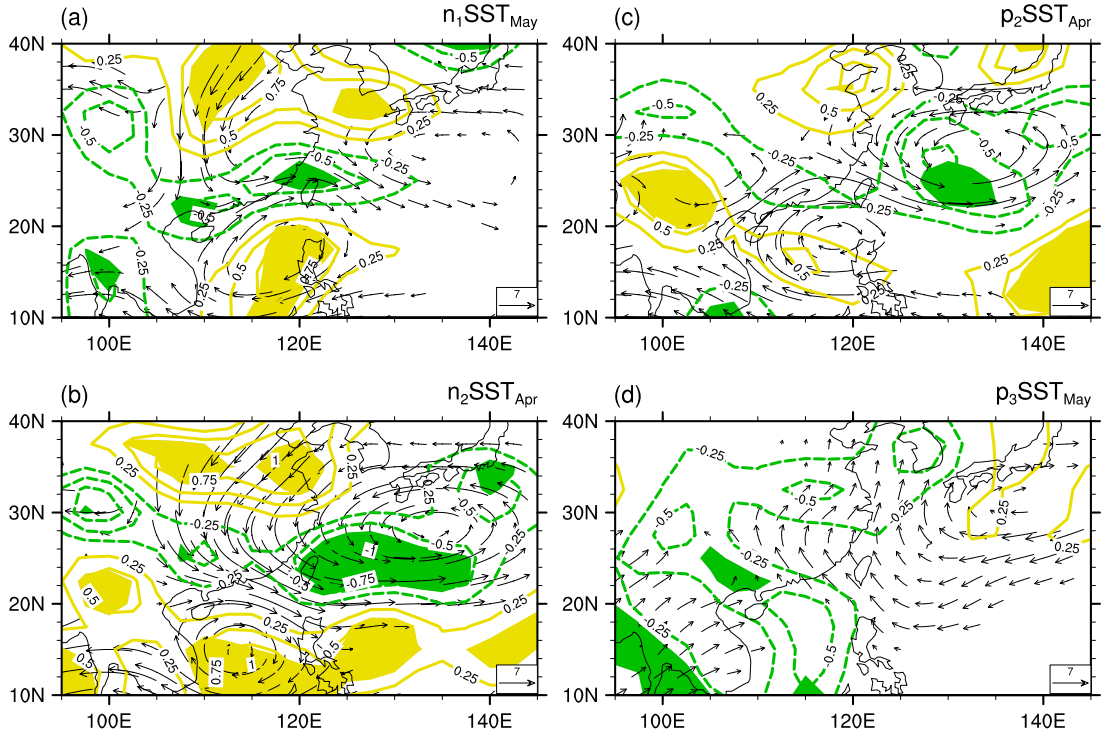

Figure 8. Regression maps for horizontal water vapor transport (vectors, unit: g kg^{-1} m s^{-1} std^{-1}) at 850 hPa and p vertical velocity (contours, unit: 10^{-2} Pa s^{-1} std^{-1}) at 500 hPa on the standardized time series of the chosen SST predictors in negative (1948–1976, left) and positive (1977–1998, right) phases of the PDO. (a–d) The dashed green (solid yellow) contours indicate ascending (descending) anomalies. The shading in Figures 8a–8d denotes the anomalies of p vertical velocity are significant at the 90% confidence level. Only significant water vapor transport vectors at 90% confidence level are plotted.

vertical velocity at 500 hPa on the chosen SST predictors. It should be noted that the regression coefficients are presented with the opposite signs for the predictors with negative correlations. The figures illustrate that in the negative PDO phase, when n_1SST$_{\mathrm{May}}$ becomes anomalously cold, an anomalous anticyclone occurs over the SCS (Figure 8a). At 500 hPa, the SC region is characterized by strongly anomalous ascending motion (Figure 8a), which drives the southwesterly transported moisture upward and leads to increased rainfall over SC. For n_2SST$_{\mathrm{Apr}}$, when the SST in this region is warmer than normal, there is also an anomalous anticyclone over the SCS and another significant cyclonic circulation from southern Japan to the Philippine Sea (Figure 8b). In addition, SC is dominated by an anomalous ascent (Figure 8b). In the positive PDO phase, when the p_2SST$_{\mathrm{Apr}}$ is warmer than normal, an anomalous anticyclone is observed over the SCS and SC is dominated by significant moist southwesterly winds (Figure 8c). Thus, more moisture will be transported from the SCS to the SC region and then concur with anomalous ascending motion there (Figure 8c). For p_3SST$_{\mathrm{May}}$, the moisture resource is from the Philippine Sea instead of the SCS (Figure 8d). Correspondingly, one can also observe a large extent of ascending anomalies over the entire East China. All of these atmospheric circulations induced by the variations of the chosen SST predictors are favorable for increasing the interannual early summer SCR. On the contrary, when the SST changes with a tendency opposite to that as described above, the induced atmospheric circulation anomalies could lead to reducing early summer SCR (figures not shown). From these analyses, it is obvious that the identified SST predictors are closely associated with the interannual variations of early summer SCR.

6. Discussion

[30] In the present study, we demonstrate that there are differences between the SST-related predictors of the early summer SCR in the PDO negative phase and those in the positive phase and suggest that the PDO may modulate the predictability of the interannual variability of the early summer SCR. However, the possible effect of ENSO change on the early summer SCR may make the PDO influences confusing. Moreover, the possible physical mechanism for the connection of PDO and SCR are still unclear. In the following, we will discuss this issue.

[31] To investigate ENSO influence on the relationship between the interannual early summer SCR and preceding SST anomalies in negative and positive PDO phases, partial correlation method [e.g., *Johnston*, 1978; *Ashok et al.*, 2003], which is often used to find correlation between two variables after removing the effects of another variable, is imported to describe the relationship between the interannual early summer SCR and preceding SST anomalies by taking away the effects of ENSO (Figure 9). It should be noted that the SST fields that correlated with the interannual Niño 3.4 index have been taken away by linear regression method before calculating the correlation coefficients. As shown in Figure 9, without the effect of ENSO, the remarkable difference of

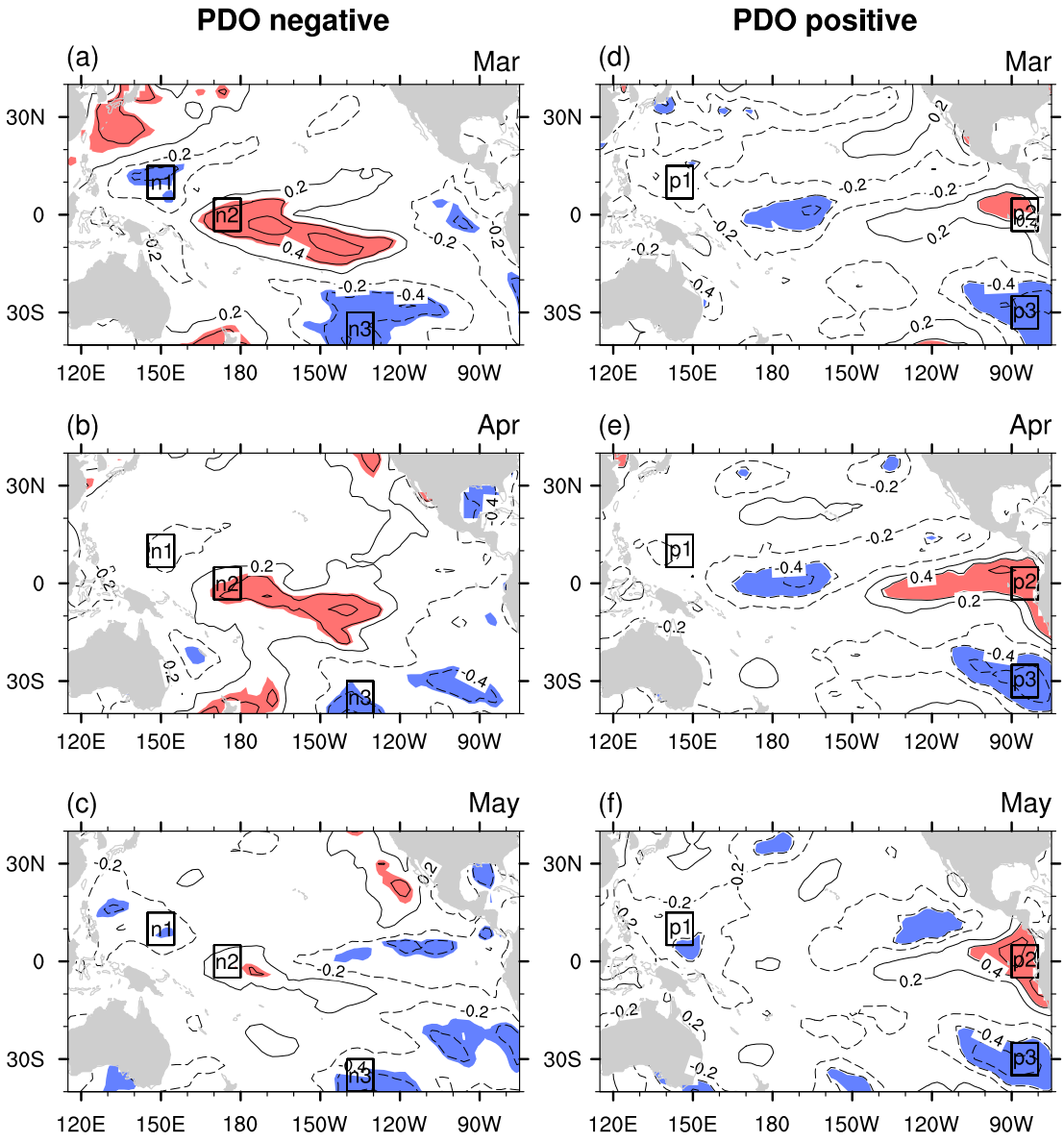

Figure 9. Partial correlation between the interannual early summer SCR and the preceding Pacific SST for (left) negative and (right) positive phases of the PDO in the training periods: 1948–1968 and 1977–1992, after removing the ENSO signals (indicated by Niño 3.4 index). Shadings indicate correlation coefficient significant at the 90% confidence level. The Niño 3.4 index (area-averaged SST anomalies over a box of 5°S–5°N and 170°W–120°W) is generally used to characterize the ENSO variability.

interannual early SCR-SST relationship between different PDO phases still apparently exists. For example, in the negative PDO phase, one can observe positive correlation in the equatorial central Pacific and negative correlation in the eastern Pacific. While in the positive PDO phase, there occurs significant positive correlation in the equatorial eastern Pacific. As a result, removing the ENSO effect cannot destroy the different SCR-SST relationship, which indicates that the PDO does modulate the interannual variability of the early summer SCR no matter remaining or removing the ENSO influence. Then what is the mechanism of the PDO affecting the interannual SCR?

[32] *Kumar et al.* [2013] suggested that the SST anomalies associated with the PDO may not have any significant feedback on the atmospheres. However, a recent study of *Krishnamurthy and Krishnamurthy* [2013] has proposed a hypothesis to illustrate the mechanism through which PDO could influence the South Asian summer monsoon. They suggest that the PDO could affect the monsoon rainfall through the seasonal footprinting of SST [*Vimont et al.*, 2001, 2003] from the North Pacific to the subtropical Pacific and further through the Walker and Hadley circulations. Here, we follow the idea of *Krishnamurthy and Krishnamurthy* [2013] to explore the possible physical mechanism for the connection of PDO and SCR. The regression pattern of preceding December, January, and February (DJF) sea level pressure (SLP) in Figure 10a displays an obvious low pressure associated with the PDO in the North Pacific, indicating an enhanced Aleutian low. The corresponding DJF SST pattern shows negative anomalies in the

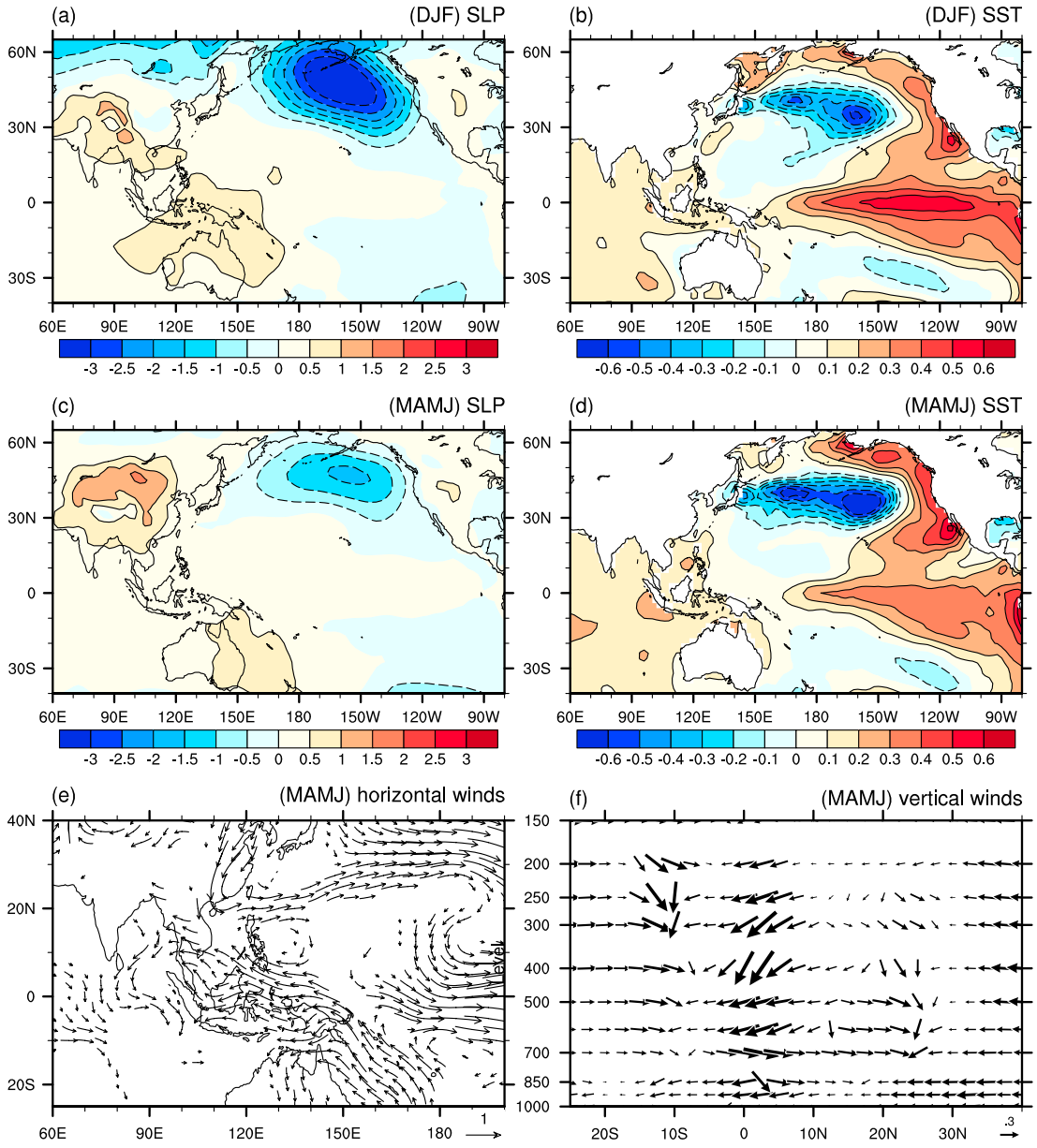

Figure 10. Anomalies of (a) SLP, (b) SST in preceding DJF (December–February averaged), and (c) SLP, (d) SST, (e) horizontal winds at 850 hPa, and (f) vertical circulations averaged over 90°E–120°E in simultaneous MAMJ (March–June averaged), respectively, regressed upon the MAMJ PDO index. In Figure 10f, the vertical wind is calculated using meridional wind and p vertical velocity from 1000 hPa to 150 hPa, and the p vertical velocity have been multiplied by −100. The units of SLP are in hPa, SST in °C, and meridional winds in m $s^{-1}$and p vertical velocity in Pa s^{-1}.

central North Pacific and positive anomalies in the equatorial eastern-central Pacific (Figure 10b). The positive SST anomalies in the equatorial Pacific persist into the next spring and early summer through the SST footprinting (Figure 10d) while the corresponding SLP negative anomalies in the North Pacific are weakened (Figure 10c). Furthermore, one can see that the equatorial westerly trade winds in the tropical central Pacific are strengthened (Figure 10e), which is associated with the persisting SST warming in the equatorial Pacific. The enhanced westerly trade winds may affect the Walker circulation with an ascending motion over the central equatorial Pacific and a complementary descending motion over the Maritime Continent (Figure 10f). At the same time, the descending anomalies can also be observed over the SC region at about 20°N–28°N (Figure 10f). Moreover, low-level anomalous northerly flows prevail over the SC region at both 850 hPa and 1000 hPa (Figures 10e and 10f). As a result, it leads to reduced rainfall over SC in the positive PDO phase. The reverse is true when PDO in its negative phase. On the other hand, the descending motion over SC may imply an intensified and southward and westward extended western Pacific subtropical high (WPSH), as the SST warming in the tropical Indian Ocean (Figures 10b and 10d) could partly explain the change of WPSH [*Zhou et al.*,

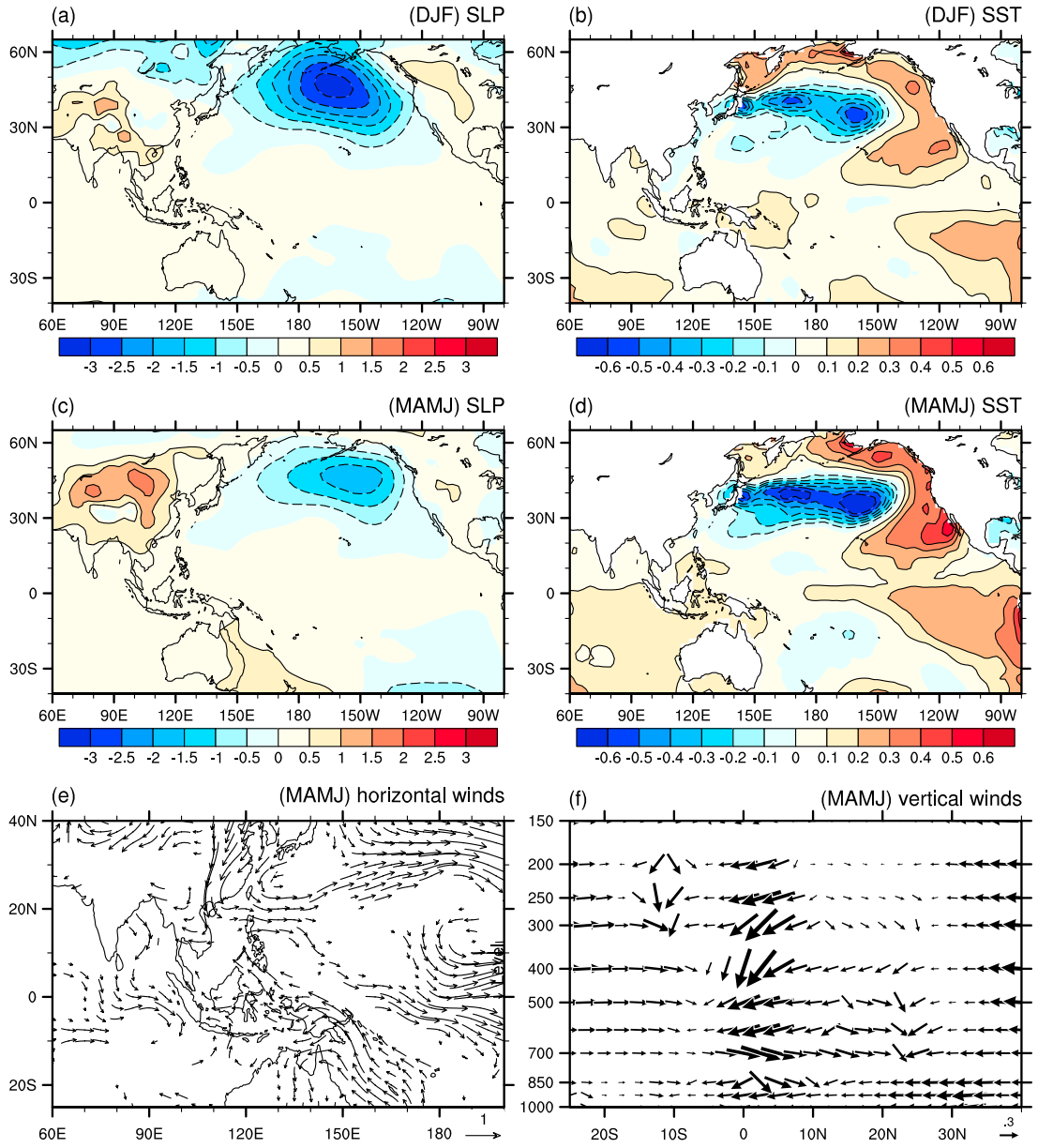

Figure 11. Same as Figure 10 but for patterns after linear removing the preceding DJF ENSO influence.

2009]. It has been demonstrated that East Asian climate anomalies are sensitive to the intensity and location of WPSH. The intensification and westward extension of WPSH (i.e., the WPSH sitting closer to East Asia) in the positive PDO phase might be responsible for the interannual early summer SCR being more predictable in the periods of PDO positive phase compared to the PDO negative phase. From these discussions on the physical mechanism of PDO influencing interannual summer SCR, it may also support the viewpoint that the PDO modulates the interannual variation of early summer SCR. Moreover, the possible physical mechanism in terms of regression patterns in Figure 10 for the connection of PDO and SCR is largely independent of the preceding DJF ENSO (Figure 11). Although the connection of PDO and SCR is largely independent of the preceding DJF ENSO, it does not say that the ENSO has no influence on the interannual variability of early summer SCR. Indeed, the removing preceding ENSO effect does weaken the SCR-SST relation in tropical regions, indicating the ENSO influence may be superimposed in the modulation of the PDO.

7. Summary

[33] In this study, we have investigated the modulation of PDO on the interannual early summer South China rainfall (SCR) with attempts to hindcast the interannual early summer SCR by considering the preceding SST anomalies. It is found that the correlation of the interannual early summer SCR with the preceding SST over the Pacific Ocean are remarkably different in the two PDO phases. When the PDO is in its positive phase, the interannual early summer SCR is closely connected to the preceding SST anomalies over tropical eastern Pacific, covering the Niño 1+2 and Niño 3 regions. However, this ENSO-like SST anomaly disappears

in the negative PDO phase, but with positive correlations over the tropical central Pacific. Although negative correlations between the interannual early summer SCR and the preceding SST anomalies can be observed in the subtropical western North Pacific region in both the positive and negative PDO phases, the corresponding high-correlation region is relatively broader for the former than for the latter.

[34] According to the correlation patterns between the interannual early summer SCR and the preceding SST, the preceding SST anomalies in several high-correlation regions are selected as potential predictors of the interannual early summer SCR for the negative and positive PDO phases, respectively. Based on these predictors, two statistical forecasting models for the interannual early summer SCR are established using respective multiple linear regressions (MLR) approach, with one model related to the negative PDO phase and the other associated with the positive PDO phase. Hindcast experiments are conducted for the interannual early summer SCR forecasting. Results suggest that the predictability of the early summer SCR in the positive PDO phase could be stronger than that in the negative PDO phase. As such, the predictability of the early summer SCR is significantly modulated by the PDO.

[35] The possible mechanism by which the PDO could influence the rainfall over SC is examined following the idea of *Krishnamurthy and Krishnamurthy* [2013]. It is hypothesized that the wintertime SST warming anomalies over the subtropical North Pacific generated by the concurrent positive PDO-related low-pressure anomalies could persist into the next spring and summer via the so-called "seasonal footprinting mechanism" [*Vimont et al*., 2001, 2003]. These SST warming anomalies could in turn force a pattern of atmospheric circulation anomalies including westerly wind anomalies along the equatorial Pacific, which subsequently weaken the Walker Circulation with an ascending motion over the central equatorial Pacific and a complementary descending motion over both the Maritime Continent and SC region. As a result, it leads to reduced rainfall over SC. On the other hand, the descending motion over SC may imply an intensified and southward and westward extended WPSH, which might be responsible for the interannual early summer SCR being more predictable in the periods of positive PDO phase. Therefore, the PDO modulates the interannual variability of the early summer SCR by modifying the Pacific SST.

[36] The rainfall forecast is difficult. It is well known that current numerical climate models generally have low forecasting skill for rainfall, compared to other key variables such as SST and mean sea level pressure. A statistical-downscaling approach may be useful for forecasting seasonal rainfall if the model simulated changes in the key variables are believed to be more reliable than the rainfall estimates themselves [e.g., *Benestad*, 2001]. This paper uses statistical forecasting models to show the predictability of the interannual early summer SCR is modulated by negative and positive PDO phases. Further work will investigate the skill of forecasting interannual rainfall by using the simulated SST from climate models through a segmented statistical-downscaling model.

[37] **Acknowledgments.** We thank the three anonymous reviewers and Dr Phil Kokic for their constructive suggestions and comments, which lead to a significant improvement in the manuscript. This work was sponsored by the National Basic Research Program of China (2010CB950400 and 2012CB955202). This work was initiated when YL visited IAP, CAS in 2012. YL is grateful for the support provided by CAS-CSIRO Exchange Program for that visit and for the support from CSIRO Climate Adaptation Flagship.

References

Ashok, K., Z. Guan, and T. Yamagata (2003), Influence of the Indian Ocean dipole on the Australian winter rainfall, *Geophys. Res. Lett.*, *30*(15), 1821, doi:10.1029/2003GL017926.

Benestad, R. E. (2001), A comparison between two empirical downscaling strategies, *Int. J. Climatol.*, *21*, 1645–1668.

Chan, J. C. L., and W. Zhou (2005), PDO, ENSO and the early summer monsoon rainfall over south China, *Geophys. Res. Lett.*, *32*, L08810, doi:10.1029/2004GL022015.

Chen, J.-M., and H.-S. Chen (2011), Inter-decadal variability of summer rainfall in Taiwan associated with tropical cyclones and monsoon, *J. Clim.*, *24*(22), 5786–5798.

Chen, L.-T., and R. Wu (2000), Interannual and decadal variations of snow cover over Qinghai-Xizang Plateau and their relationships to summer monsoon rainfall in China, *Adv. Atmos. Sci.*, *17*, 18–30.

Davis, R. E. (1976), Predictability of sea surface temperature and sea level pressure anomalies over the North Pacific Ocean, *J. Phys. Oceanogr.*, *6*(3), 249–266.

Ding, Y.-H., Z.-Y. Wang, and Y. Sun (2008), Inter-decadal variation of the summer precipitation in East China and its association with decreasing Asian summer monsoon. Part I: Observed evidences, *Int. J. Climatol.*, *28*, 1139–1161, doi:10.1002/joc.1615.

Garreaud, R. D., and D. S. Battisti (1999), Inter-annual (ENSO) and inter-decadal (ENSO-like) variability in the Southern Hemisphere tropospheric circulation, *J. Clim.*, *12*(7), 2113–2123.

Gershunov, A., and T. P. Barnett (1998), Interdecadal modulation of ENSO teleconnections, *Bull. Am. Meteorol. Soc.*, *79*(12), 2715–2725.

Gong, D.-Y., and C.-H. Ho (2002), Shift in the summer rainfall over the Yangtze River valley in the late 1970s, *Geophys. Res. Lett.*, *29*(10), 1436, doi:10.1029/2001GL014523.

Guo, Y., J. Li, and Y. Li (2012), A time-scale decomposition Approach to Statistically Downscale Summer Rainfall over North China, *J. Clim.*, *25*(2), 572–591.

Hu, Z.-Z. (1997), Interdecadal variability of summer climate over East Asia and its association with 500 hPa height and global sea surface temperature, *J. Geophys. Res.*, *102*, 19,403–19,412.

Hu, Z.-Z., and B. Huang (2009), Interferential impact of ENSO and PDO on dry and wet conditions in the US Great Plains, *J. Clim.*, *22*(22), 6047–6065.

Hu, Z.-Z., S. W. Wang, and Z. C. Zhao (1993), Analyses of the abrupt changes of rainfall in July along lower reach of Yellow River and its causes, in *Diagnostic Study of the Rule of Droughts and Floods Happening in Regions of Yangtze River Valley and Yellow River Valley and Their Impact on Economics (in Chinese)*, edited by S. W. Wang et al., pp. 197–202 , China Meteorological Press, Beijing.

Huang, R., and W. Li (1987), Influence of the heat source anomaly over the tropical western Pacific on the subtropical high over East Asia, paper presented at Proc. International conference on the general circulation of East Asia.

Johnston, R. (1978), *Multivariate Statistical Analysis in Geography*, pp. 280, Longman, London.

Kalnay, E., et al. (1996), The NCEP/NCAR reanalysis project, *Bull. Am. Meteorol. Soc.*, *77*, 437–471, doi:10.1175/1520-0477(1996)077<0437:TNYRP>2.0.CO;2.

Kim, J.-W., S.-W. Yeh, and E.-C. Chang (2013), Combined effect of El Niño–Southern Oscillation and Pacific Decadal Oscillation on the East Asian winter monsoon, *Clim. Dyn.*, doi:10.1007/s00382-013-1730-z.

Krishnamurthy, L., and V. Krishnamurthy (2013), Influence of PDO on South Asian monsoon and monsoon-ENSO relation, *Clim. Dyn.*, doi:10.1007/s00382-013-1856-z.

Kumar, A., H. Wang, W. Wang, Y. Xue, and Z.-Z. Hu (2013), Does knowing the oceanic PDO phase help predict the atmospheric anomalies in subsequent months?, *J. Clim.*, *26*(4), 1268–1285.

Li, Y., and I. Smith (2009), A statistical downscaling model for southern Australia winter rainfall, *J. Clim.*, *22*(5), 1142–1158.

Lin, Z. D., R. Y. Lu, and W. Zhou (2010), Change in early-summer meridional teleconnection over the western North Pacific and East Asia around the late 1970s, *Int. J. Climatol.*, *30*, 2195–2204, doi:10.1002/joc.2038.

Livezey, R. E., and W. Y. Chen (1983), Statistical field significance and its determination by Monte Carlo techniques, *Mon. Weather Rev.*, *111*, 46–59.

Mantua, N. J. (2002), Pacific Decadal Oscillation, in *The Encyclopedia of Global Environmental Change, The Earth System—Physical and Chemical Dimensions of Global Environmental Change*, vol. 1, edited by M. C. McCracken and J. S. Perry, pp. 592–594, Wiley, Chichester, N. Y.

Mantua, N. J., S. R. Hare, Y. Zhang, J. M. Wallace, and R. C. Francis (1997), A Pacific inter-decadal climate oscillation with impacts on salmon production, *Bull. Am. Meteorol. Soc.*, *78*(6), 1069–1079.

Mao, J., J. C. Chan, and G. Wu (2011), Inter-annual variations of early summer monsoon rainfall over South China under different PDO backgrounds, *Int. J. Climatol.*, *31*(6), 847–862.

Miller, A. J., D. R. Cayan, T. P. Barnett, N. E. Graham, and J. M. Oberhuber (1994), The 1976–77 climate shift of the Pacific Ocean, *Oceanography*, *7*(1), 21–26.

Nitta, T. (1987), Convective activities in the tropical western Pacific and their impact on the Northern Hemisphere summer circulation, *J. Meteorol. Soc. Jpn.*, *65*(3), 373–390.

Nitta, T. (1989), Global features of the Pacific-Japan oscillation, *Meteorol. Atmos. Phys.*, *41*, 5–12, doi:10.1007/BF01032585.

Nitta, T., and Z.-Z. Hu (1996), Summer climate variability in China and its association with 500 hPa height and tropical convection, *J. Meteorol. Soc. Jpn.*, *74*, 425–445.

Power, S., T. Casey, C. Folland, A. Colman, and V. Mehta (1999), Interdecadal modulation of the impact of ENSO on Australia, *Clim. Dyn.*, *15*(5), 319–324.

Qian, W., and A. Qin (2008), Precipitation division and climate shift in China from 1960 to 2000, *Theor. Appl. Climatol.*, *93*, 1–17, doi:10.1007/s00704-007-0330-4.

Silva, G. A. M., A. Drumond, and T. Ambrizzi (2011), The impact of El Niño on South American summer climate during different phases of the Pacific Decadal Oscillation, *Theor. Appl. Climatol.*, *106*, 307–319.

Smith, T. M., R. W. Reynolds, T. C. Peterson, and J. Lawrimore (2008), Improvements to NOAA's historical merged land-ocean surface temperature analysis (1880–2006), *J. Clim.*, *21*(10), 2283–2296.

Vimont, D. J., D. S. Battisti, and A. C. Hirst (2001), Footprinting: A seasonal connection between the tropics and midlatitudes, *Geophys. Res. Lett.*, *28*, 3923–3926.

Vimont, D. J., D. S. Battisti, and A. C. Hirst (2003), The seasonal footprinting mechanism in the CSIRO general circulation models, *J. Clim.*, *16*, 2653–2667.

Wang, B., R. Wu, and X. Fu (2000), Pacific-East Asian teleconnection: How does ENSO affect East Asian climate?, *J. Clim.*, *13*(9), 1517–1536.

Wu, R., and L.-T. Chen (1998), Decadal variation of summer rainfall in the Yangtze-Huaihe River valley and its relationship to atmospheric circulation anomalies over East Asia and western North Pacific, *Adv. Atmos. Sci.*, *15*, 510–522.

Wu, R., Z.-P. Wen, S. Yang, and Y.-Q. Li (2010), An interdecadal change in southern China summer rainfall around 1992–93, *J. Clim.*, *23*, 2389–2403.

Wu, R., S. Yang, Z. Wen, G. Huang, and K. Hu (2012), Inter-decadal change in the relationship of southern China summer rainfall with tropical Indo-Pacific SST, *Theor. Appl. Climatol.*, *108*(1), 119–133.

Xue, F., and J. He (2005), Influence of the Southern Hemispheric circulation on east-west oscillation of the western Pacific subtropical high, *Chin. Sci. Bull.*, *50*(14), 1532–1536.

Xue, F., H. Wang, and J. He (2003a), Inter-annual variability of Mascarene high and Australian high and their influences on summer rainfall over East Asia, *Chin. Sci. Bull.*, *48*(5), 492–497.

Xue, F., D. Jiang, X. Lang, and H. Wang (2003b), Influence of the Mascarene high and Australian high on the summer monsoon in East Asia: Ensemble simulation, *Adv. Atmos. Sci.*, *20*(5), 799–809.

Yatagai, A., and T. Yasunari (1994), Trends and decadal-scale fluctuations of surface air temperature and precipitation over China and Mongolia during the recent 40 year period (1951–1990), *J. Meteorol. Soc. Jpn.*, *72*, 937–957.

Zhang, H., J. Qin, and Y. Li (2011), Climatic background of cold and wet winter in southern China: Part I. Observational analysis, *Clim. Dyn.*, *37*(11), 2335–2354.

Zhang, Y., J. M. Wallace, and D. S. Battisti (1997), ENSO-like inter-decadal variability: 1900–93, *J. Clim.*, *10*(5), 1004–1020.

Zhang, Y., T. Li, and B. Wang (2004), Decadal change of the spring snow depth over the Tibetan Plateau and influence on the East Asian summer monsoon, *J. Clim.*, *17*, 2780–2793.

Zhou, T., R. Yu, J. Zhang, H. Drange, C. Cassou, C. Deser, D. L. Hodson, E. Sanchez-Gomez, J. Li, and N. Keenlyside (2009), Why the western Pacific subtropical high has extended westward since the late 1970s, *J. Clim.*, *22*(8), 2199–2215.

Zhou, W., and J. C. L. Chan (2007), ENSO and South China Sea summer monsoon onset, *Int. J. Climatol.*, *27*, 157–167.

Zhou, W., C. Li, and J. Chan (2006), The inter-decadal variations of the summer monsoon rainfall over South China, *Meteorol. Atmos. Phys.*, *93*(3), 165–175.

Zhou, W., X. Wang, T. Zhou, C. Li, and J. Chan (2007), Inter-decadal variability of the relationship between the East Asian winter monsoon and ENSO, *Meteorol. Atmos. Phys.*, *98*(3-4), 283–293.

Zhu, Y. L., H. J. Wang, W. Zhou, and J. H. Ma (2011), Recent changes in the summer precipitation pattern in east China and the background circulation, *Clim. Dyn.*, *36*, 1463–1473, doi:10.1007/s00382-010-0852-9.